Direct and GTP-dependent interaction of ADP ribosylation factor 1 with coatomer subunit β

Liyun Zhao*, J. Bernd Helms*, Britta Brügger*, Cordula Harter*, Bruno Martoglio†, Roland Graf‡, Josef Brunner‡, and Felix T. Wieland*§

*Biochemie-Zentrum Heidelberg, Universität Heidelberg, Im Neuenheimer Feld 328, D-69120 Heidelberg, Germany; †Zentrum für Molekulare Biologie Heidelberg, Im Neuenheimer Feld 282, D-69120 Heidelberg, Germany; and ‡Laboratorium für Biochemie, Eidgenössische Technische Hochschule Zürich, Universtitätstrasse 16, CH-8092 Zürich, Switzerland

ABSTRACT   A site-directed photocrosslink approach was used to elucidate components that interact directly with ADP-ribosylation factor (ARF)-GTP during coat assembly. Two ARF mutants were generated that contain a photolabile amino acid at positions distant to each other within the ARF molecule. Here we show that one of the two positions specifically interacts with coatomer subunit β both on Golgi membranes and in isolated coat protein complex type I (COPI)-coated vesicles. Thus, a direct and GTP-dependent interaction of coatomer via β-coat protein complex (COP) with ARF is involved in the coating of COPI-coated vesicles. These data implicate a bivalent interaction of the complex with the donor membrane during vesicle formation.

COPI-coated vesicles are thought to mediate the transport of proteins across the Golgi stack (1, 2) and between the Golgi and the endoplasmic reticulum (3). Budding of these vesicles from the Golgi includes GTP-dependent binding to the membranes of the small G protein ADP-ribosylation factor (ARF) and subsequent recruitment of a cytosolic protein complex, coatomer (4, 5), leading to the formation of buds and vesicles as shown by *in vitro* experiments (6). Recently, the cytosolic tail sequence motif KKXX-COOH of type I transmembrane proteins has been implicated in coatomer binding (7), and it was shown that coatomer subunits bind directly to this motif (7–9). To determine the specific role of ARF in the recruitment of the coat, we have used a site-directed photocrosslink approach to elucidate components that interact directly with ARF-GTP during coat assembly. The three-dimensional structure of ARF-GDP has recently been described (10). Given that binding of ARF involves its *N*-myristic acid residue (5, 11), the most likely orientation of the ARF molecule toward membranes is as depicted in Fig. 1. Dismissing major structural differences between the GDP and GTP forms of ARF (as deduced from other members of the G-protein family; ref. 13) we selected the positions of Phe-13 and Phe-82 to incorporate a photolabile analog of phenylalanine, trifluoromethyldiazirino-phenylalanine (Tmd-Phe) (14, 15), because these positions are distant from each other; one close to the membrane and the other exposed to the cytosol, and thus likely to react with different partners.

MATERIALS AND METHODS

Construction and *in Vitro* Translation of Site-Specific Photolabile ARF Mutants. The three-dimensional structure of

ARF1 has been described by Amor *et al*. (10). ARF1 was depicted using the WHATIF program (16). For introduction of the photolabile amino acid L-4′-(3-trifluoromethyl-3*H*-diazirin-3-yl)phenylalanine [(Tmd)Phe], the amber stopcodon (TAG) was introduced into the coding region of the ARF cDNA by replacement with codon 13 [ARF-(Tmd)Phe-13] or 82 [ARF-(Tmd)Phe-82] into the plasmid pET-11d containing the ARF cDNA (17) by PCR. Amber suppressor tRNA was synthesized as described (14, 18). *In vitro* transcription using T7 RNA polymerase and *in vitro* translation using Flexi-lysate (Promega) was performed with linearized plasmids according to the manufacturer's protocol. After *in vitro* translation (in the presence or absence of 5 μM suppressor tRNA) for 2 hr at 30°C, a sample was taken from the incubation and analyzed by SDS/PAGE (19) and subsequent autoradiography (Fig. 2*a*). For the experiments described in Fig. 2*b*, [^{35}S]methionine-labeled ARF was partially purified from the lysate by gel filtration. One milliliter of lysate was fractionated on a Biogel P-60 column (Bio-Rad, 1 × 50 cm) in 25 mM Hepes/KOH (pH 7.2), 2.5 mM Mg(OAc)$_2$, and 20 mM KCl and the ARF-containing fractions were pooled and stored at 0°C until use. wild-type [^{35}S]ARF (42,000 cpm), [^{35}S]ARF-(Tmd)Phe-13 (65,000 cpm), or [^{35}S]ARF(Tmd)Phe-82 (17,000 cpm) was incubated with 2 μg of isolated CHO Golgi membranes (20) in 25 mM Hepes/KOH (pH 7.2), 20 mM KCl, 2.5 mM Mg(OAc)$_2$, ovalbumin (1 mg/ml), 0.2 M sucrose, and 50 μM nucleotide {guanosine 5′-[β-thio]diphosphate (GDP[βS]) or guanosine 5′-[γ-thio]triphosphate (GTP[γS]), as indicated in the figures} in a total volume of 50 μl for 15 min at 37°C. The binding reaction was stopped by transferring the incubations to ice. The reaction mixture was loaded onto a 175 μl cushion of 15% sucrose (wt/vol) in 25 mM Hepes/KOH (pH 7.2), 20 mM KCl, and 2.5 mM Mg(OAc)$_2$ in a 0.5 ml tube and centrifuged for 30 min at 14,000 rpm (4°C). For the experiments shown in Fig. 2*b*, the membrane pellet was solubilized in 40 μl of 0.5% Triton X-100 in PBS, and radioactivity was determined by liquid scintillation counting. The amount of binding in the presence of GTP[γS] is set to (100%). Typically this corresponded to 1,000–1,500 cpm after substraction of a background (incubation without membranes, $\approx$100 cpm).

Photocrosslinking of the ARF Mutants. *In vitro*-translated ARF-(Tmd)Phe-13 and ARF-(Tmd)Phe-82 was partially purified as described above. Incubations were as described in legend to Fig. 2, except that the total incubation was increased 10-fold to 500 μl. After incubation the Golgi membranes were pelleted in a microcentrifuge (30 min at 14,000 rpm at 4°C) and

Cell Biology: Zhao *et al.*

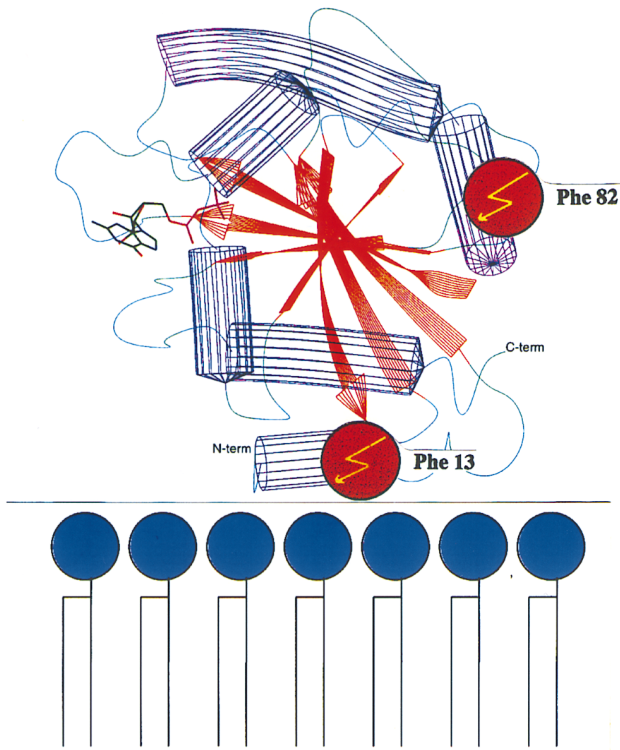*Proc. Natl. Acad. Sci. USA* 94 (1997)   4419

FIG. 1.   Localization of Phe-13 and Phe-82 within the ARF molecule. A schematical drawing of ARF1, highlighting the location of phenylalanine at amino acid positions 13 and 82. The orientation of ARF1, relative to the membrane, is based on the requirement for stable membrane binding of a myristic acid residue, covalently bound to the N-terminal Gly-2 of ARF (11). The alkyl chain likely functions as an anchor for binding of ARF to the membranes (11, 12)

resuspended in 20 μl of 25 mM Hepes/KOH (pH 7.2), 20 mM KCl, 2.5 mM Mg(OAc)$_2$ and 0.2 M sucrose. When no membranes were present during the incubation (lane 5), the total volume of incubation was 50 μl and these samples were not subjected to centrifugation but rather the complete incubation was subjected to irradiation. Samples were irradiated at 366 nm for 2 min on ice (15), and thereafter the proteins were precipitated with trichloroacetic acid and analyzed by SDS/PAGE (19) (lanes 1–9 represent a 12% acrylamide gel and lanes 10–12 represent a linear gradient gel containing 7.5–15% acrylamide) and subsequent autoradiography. Coatomer was purified as described (21). Recombinant mARF1 was produced and purified as described by Weiss *et al.* (22). ARF-depleted cytosol was prepared by gel-filtration of CHO-cytosol (20) on Biogel P60 (Bio-Rad). Coatomer-containing fractions (as determined by Western blot analysis using antibodies against various subunits) that are devoid of ARF (as determined by Western blot analysis using an anti-ARF1 antibody; ref. 5) were pooled, dialyzed against 25 mM Tris·HCl (pH 7.4), 50 mM KCl, and 1 mM DTT, concentrated to 24 mg/ml, and frozen at −80°C. In incubations with cytosol the final concentration was 2.4 mg/ml. It is of note that to see the crosslink product, the autoradiogram needs to be overexposed with respect to the ARF band (at a molecular mass of 21 kDa). Due to this overexposure, the difference of, for example, the signals produced by the amount of ARF bound in the presence of GTP[γS] vs. GDP[βS] (lanes 2 and 4, respectively) is not as pronounced as in Fig. 2*b*. However, at shorter exposures the ratio of the ARF bound in the presence of GTP[γS] vs. GDP[βS] is similar to that of Fig. 2*b* (data not shown).

Antibodies and Immunoprecipitation. In case the proteins were denatured prior to immunoprecipitation, SDS was added to a final concentration of 1% and the samples (20 μl) were
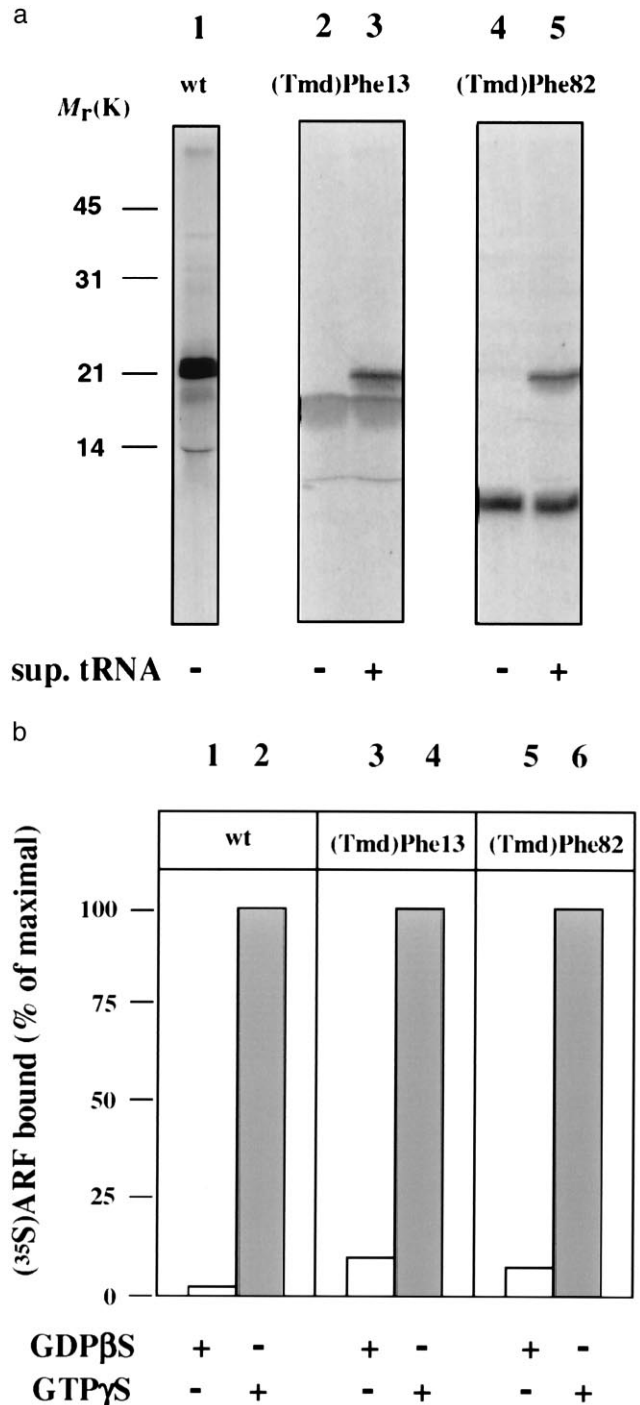

FIG. 2.   Characterization of incorporation of (Tmd)Phe into ARF protein. (*a*) Autoradiograph of an SDS/polyacrylamide gel of [^{35}S]methionine-labeled products from *in vitro* translations of wild-type (wt) ARF1 (lane 1), ARF-(Tmd)Phe-13 (lanes 2 and 3), and ARF-(Tmd)Phe-82 (lanes 4 and 5) both in the absence (lanes 2 and 4) and presence (lanes 3 and 5) of suppressor tRNA; (*b*) *in vitro*-translated wt-ARF (lane 1 and 2), ARF-(Tmd)Phe-13 (lane 3 and 4), and ARF-(Tmd)Phe-82 (lane 5 and 6) were incubated with isolated Golgi membranes from Chinese hamster ovary (CHO) cells in the presence of GDP[βS] (lanes 1, 3, and 5) or GTP[γS] (lanes 2, 4, and 6). After incubation, the amount of radioactivity associated with the membranes was determined.

incubated for 3 min at 95°C. For immunoprecipitation, the samples were added to 250 μl of 20 mM Tris·HCl (pH 7.5), 2 mM EDTA, 0.15 M NaCl, and 0.5% Triton X-100 (immunoprecipitation buffer). If SDS was present in the sample, the

amount of Triton X-100 was increased to 0.9% to have a 10-fold excess of Triton X-100 over SDS. The samples were solubilized for 2 hr at 4°C by head-over-head rotation and subsequently incubated with the indicated antibodies, coupled to protein A Sepharose (Pharmacia) for 2 hr at 4°C by head-over-head rotation. The beads were washed five times in IP buffer and once in PBS. The immunoprecipitated material was solubilized in sample buffer and analyzed by SDS/PAGE (18) and autoradiography. For immunoprecipitation, antibodies against the whole coatomer complex (anti-CM1; ref. 5), and antibodies against the individual subunits, β'-coat protein complex (COP) (23), γ-COP (polyclonal rabbit antiserum directed against recombinant γ-COP protein; ref. 9), and β-COP (24) were used. Western blot analysis (25) and subsequent immunodetection of the coatomer subunits was performed with the following antibodies: anti-α/γ-COP (26), anti-β'-COP (27), and anti-β-COP (mAb M3A5; ref. 28). For visualization the enhanced chemiluminescence system (Amersham) was used.

Generation of Coat Protein Complex Type I (COPI)-Coated Vesicles with [³⁵S]ARF-(Tmd)Phe. COPI-coated vesicles were generated from CHO Golgi membranes by incubation of Golgi membranes with cytosol and GTP[γS], in principle as described by Serafini *et al.* (12). To avoid dilution of *in vitro*-translated [³⁵S]ARF-(Tmd)Phe-82 (0.5 ml of lysate, 8.5×10^6 dpm) with the large cytosolic pool of nonradiolabeled ARF, isolated CHO Golgi membranes were incubated for 5 min with the radiolabeled ARF in a complete incubation but omitting bovine brain cytosol (during which time no vesicles can form due to the absence of the cytosolic component coatomer). The incubation was then continued for 20 min in the presence of cytosol (total volume of incubation was 60 ml). After centrifugation, the membranes were resuspended in 0.6 ml of low salt

buffer (29). Nonspecifically bound ARF (30) was removed from the membranes by extraction of the membranes with 8.2 ml of 6 mM phosphatidylcholine liposomes; ref. 30). Under these conditions, 50% of [³⁵S]ARF-(Tmd)Phe-82 radioactivity was removed from the membranes (data not shown). The membranes were pelleted for 30 min at $14,000 \times g$ at 4°C and resuspended in high salt buffer (29). Further procedures for isolation of COPI-coated vesicles from the high salt solution and subsequent sucrose density gradient centrifugation were according to Malhotra *et al.* (29). Fractions of 250 μl were collected from the gradient (fraction 1 representing the highest sucrose density). The radioactivity present in each fraction was determined by liquid scintillation counting of 10 μl aliquots. For the experiments shown in Fig. 5c, the gradient fractions were irradiated at 366 nm for 2.5 min on ice prior to precipitation of the proteins with trichloroacetic acid and analysis by SDS/PAGE and subsequent autoradiography (Fig. 5 c and d) or subsequent immunoblotting (Fig. 5b) using an anti-ARF1 antibody (5) and an anti-β-COP antibody (EAGE) (31).

RESULTS

To generate ARF mutants that were site-specifically photolabeled at positions Phe-13 and Phe-82, the corresponding codons of the ARF1 cDNA were mutated to amber, and, as shown in Fig. 2a, these stopcodons could be repressed in an *in vitro* transcription-translation assay in the presence of [³⁵S]methionine, using suppressor tRNA loaded with Tmd-Phe (14, 18).

The radioactive and photolabile ARF proteins were purified by gel filtration and probed for their ability to bind to Golgi membranes in an GTP[γS]-dependent manner (12, 30, 32). As shown in Fig. 2b, both ARF mutants exhibit a GTP[γS]-
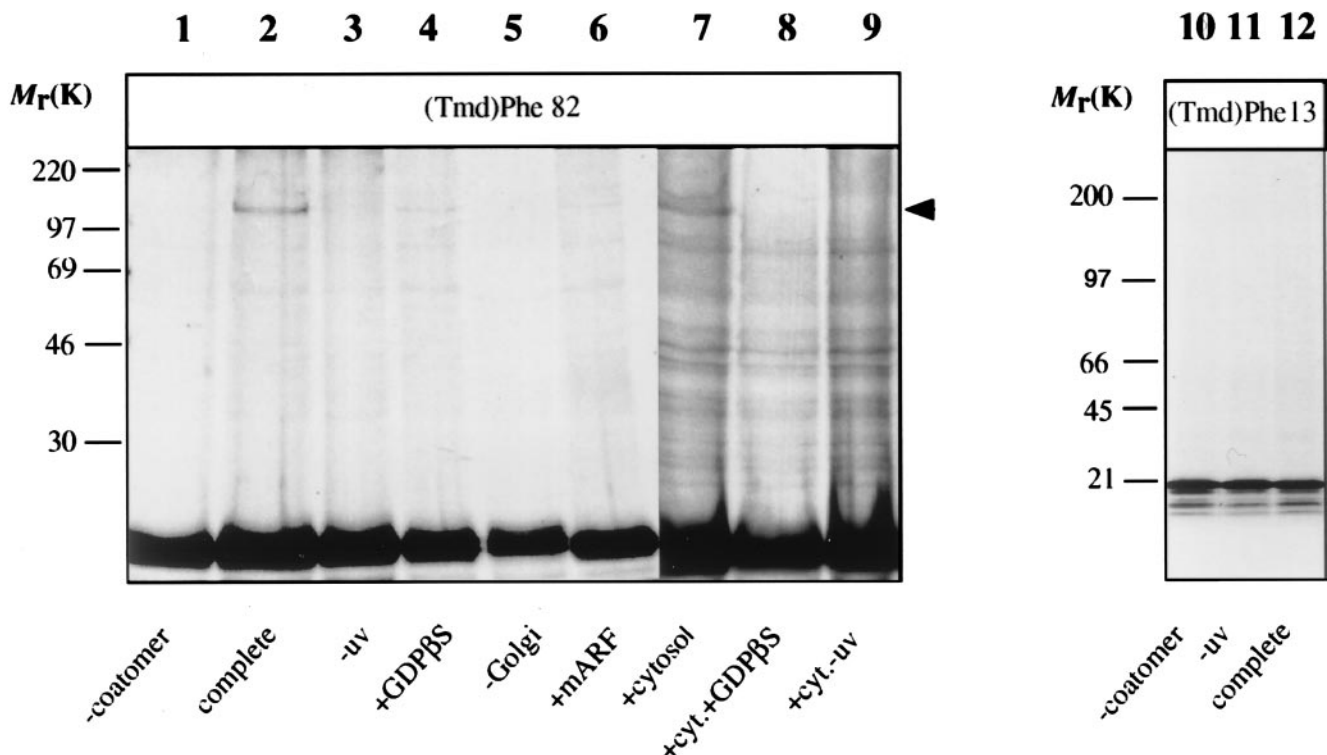

FIG. 3. Photocrosslinking of membrane-bound [³⁵S]ARF-(Tmd)Phe-13 and [³⁵S]ARF-(Tmd)Phe-82. *In vitro*-translated ARF-(Tmd)Phe-82 (lanes 1–9) and ARF-(Tmd)Phe-13 (lanes 10–12) was incubated in the absence (lane 5) or presence (all other lanes) of Golgi membranes, with GDP[βS] (lanes 4 and 8) or GTP[γS] (all other lanes), in the absence (lanes 1 and 7–10) or presence (all other lanes) of purified coatomer, in the presence of an excess of myristoylated ARF1 (lane 6) or in the presence of ARF-depleted cytosol (lanes 7–9). After incubation the samples were centrifuged and the membranes were irradiated (except lanes 3, 9, and 11) and membrane-bound material was analyzed by SDS/PAGE (19) and autoradiography. When no membranes were present during the incubation (lane 5), the complete incubation (but in 50 μl) was irradiated (without prior centrifugation) and was analyzed by SDS/PAGE and autoradiography.

Cell Biology: Zhao *et al.*

Proc. Natl. Acad. Sci. USA 94 (1997) 4421

dependent binding similar to the wild-type ARF. These mutants were then used in a photocrosslink approach to identify possible partners that directly interact with ARF-GTP[γS]. Isolated Golgi membranes were incubated with the ARF mutant proteins under the various conditions indicated in Fig. 3. The membranes were recovered by centrifugation through a sucrose cushion, and subsequently the resuspended membranes were illuminated at 366 nm, and analyzed by SDS/PAGE. The results are shown in Fig. 3. In the presence of coatomer and GTP[γS] a photocrosslink product appears of [^{35}S]methionine-ARF-(Tmd)Phe-82 with an apparent molecular mass of $\approx$120 kDa (Fig. 3, lane 2). This band is not detected in the absence of coatomer and is very faint in the presence of GDP[βS] (lanes 1 and 4, respectively). Formation of the 120-kDa signal is suppressed by the addition of excess unlabeled wild-type ARF (lane 6), and does not appear when ARF-(Tmd)Phe-82 is illuminated in the presence of coatomer but in the absence of membranes (lane 5). The radiolabeled band visible in all lanes at $\approx$60 kDa is present in a control that has not been illuminated (lane 3) and is therefore regarded unspecific. An additional criterion for specificity of the interaction that led to the formation of the 120-kDa crosslink product is the pattern obtained after incubation of samples in the presence of ARF-depleted cytosol as a source of coatomer. As shown in lane 7 of Fig. 3, the addition of ARF-depleted cytosol gives rise to the same specific band (see arrowhead in Fig. 3). In addition to this 120-kDa product a variety of other bands are visible, regarded as nonspecific because their appearance is independent of irradiation (lane 9 in Fig. 3). Again, the 120-kDa signal is strongly suppressed in the presence of GDP[βS] (lane 8). In summary binding of an ARF molecule with a photolabile residue in position 82 leads to a highly specific and GTP[γS]-dependent crosslink product of $\approx$120 kDa. If this product is due to a cytosolic orientation of position 82 as postulated in Fig. 1, then a photolabile residue in a position distant to residue 82, in the membrane-oriented site of ARF, should not give rise to the same band. Therefore we have repeated the experiment with ARF-(Tmd)Phe-13, a position presumed to be in close proximity to the membrane. As a result, no crosslink products were obtained in a molecular weight range indicative of protein-interactions (Fig. 3, lanes 10–12). Even after prolonged exposition of the gel (10-fold as compared with Fig. 3, lanes 10–12) no irradiation-dependent higher molecular weight bands were observed (data not shown). However, we cannot exclude at this stage an interaction of the Phe-13 site with other membrane constituents. This is taken as strong additional evidence for the specificity of the ARF-(Tmd)Phe-82 protein interaction visualized in the 120-kDa product.

The strict dependence on the presence of coatomer suggested that the crosslink observed reflects a direct interaction of the complex with the membrane bound ARF-GTP[γS]. This was substantiated by immunoprecipitation with anti-coatomer antibodies after crosslinking, as shown in Fig. 4b, lane 2. The apparent molecular mass of the crosslinked product ($\approx$120 kDa) suggested an interaction of ARF ($\approx$21 kDa) with a member of coatomer's 100-kDa family of proteins, β-, β'-, or γ-COP. The coatomer subunit specifically crosslinked was therefore analyzed by immunoprecipitation with antibodies directed against these individual subunits. As expected, under nondissociating conditions, each of these antibodies precipitated the complete coatomer, and therefore, the 120-kDa product (Fig. 4b, lanes 3, 5, and 7). However, if the complex was dissociated before immunoprecipitation, neither the anti-γ- nor the anti-β'-COP antibodies precipitated the crosslinked product (Fig. 4b, lanes 4 and 6), although both were able to precipitate their respective antigens under the conditions used (Fig. 4a, lanes 4 and 6). In contrast, the anti-β-COP-antibodies did recognize the radiolabeled product after dissociation of coatomer (lane 8 in Fig. 4b). Thus, we conclude that in the
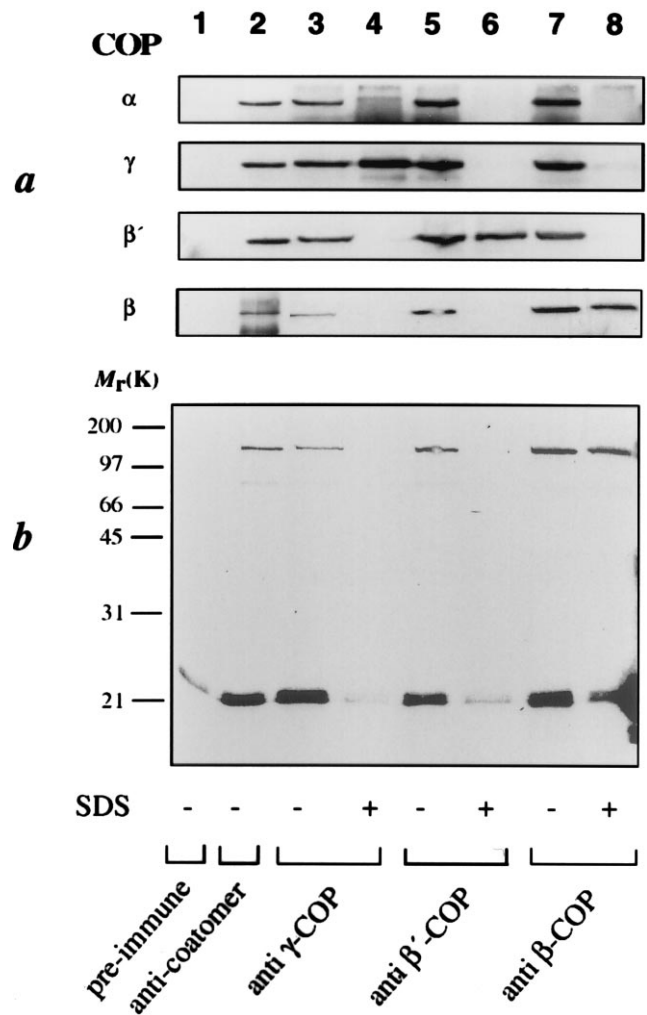

FIG. 4. Immunoprecipitation of membrane-bound coatomer and its individual subunits. *In vitro*-translated [^{35}S]ARF-(Tmd)Phe-82 was bound to CHO Golgi membranes in the presence of GTP[γS] and coatomer as described in Fig. 2, lane 2. After irradiation of membrane-bound ARF, the membranes were solubilized in detergent-buffer and the coatomer complex was immunoprecipitated using anti-coatomer-antibody (lane 2), anti-γ-COP antibody (lanes 3 and 4), anti-β'-COP antibody (lanes 5 and 6), and anti-β-COP antibody (lanes 7 and 8). In some cases, coatomer was denatured prior to immunoprecipitation to allow immunoprecipitation of the individual subunits (lanes 4, 6, and 8). Immunoprecipitation with a pre-immune serum is shown in lane 1. (*a*) As a control, immunoprecipitated material from incubations shown in *b* was analyzed for the presence of individual coatomer subunits by SDS/PAGE (19) and Western blot analysis with the respective antibodies. (*b*) Immunoprecipitated material was analyzed by SDS/PAGE (19) and autoradiography.

budding of COPI-coated vesicles a direct interaction of β-COP and ARF-GTP is involved to recruit coatomer to the Golgi membrane.

This result raised the question whether the observed interaction of β-COP with ARF is transient and needed exclusively to recruit coatomer to the Golgi membranes. If so, this interaction should not be observed in isolated COPI-coated transport vesicles. To address this question, COPI-coated vesicles were generated *in vitro* in the presence of [^{35}S]methionine-ARF-(Tmd)Phe-82 and isolated by sucrose density gradient centrifugation (29). As shown in Fig. 5a, a [^{35}S]methionine radioactivity profile was obtained with a peak at the position of COPI-coated vesicles, substantiated by immunoblotting of these fractions with antibodies directed against β-COP and ARF (see Fig. 5b). The individual fractions were
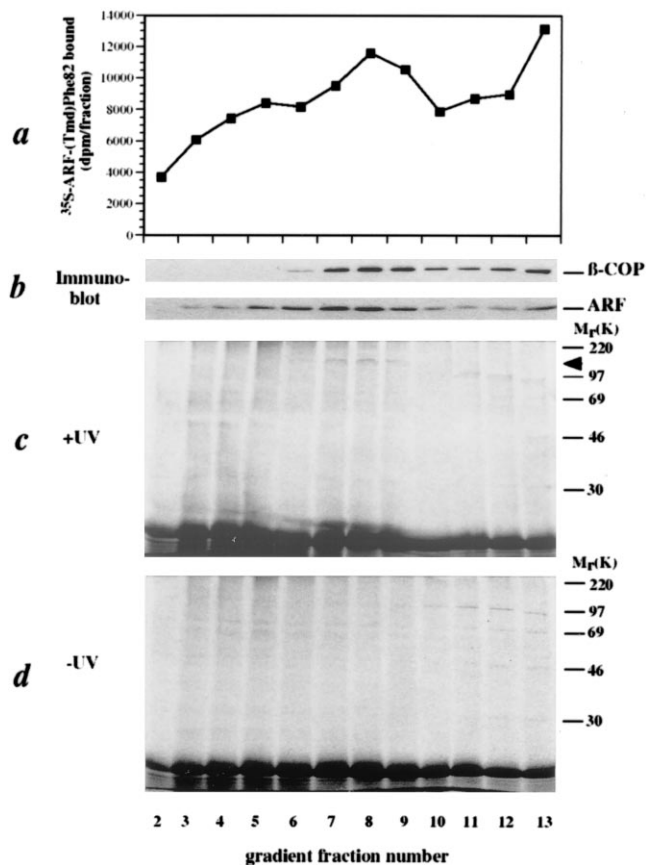
FIG. 5.   ARF interacts with β-COP in COPI-coated vesicles. In the presence of [^{35}S]ARF-(Tmd)Phe-82, isolated CHO Golgi membranes were incubated with bovine brain cytosol and GTP[γS]. The COPI-coated vesicles were separated from their donor membranes by sucrose density gradient centrifugation and the gradients were fractionated. (*a*) The amount of total ^{35}S radioactivity present in each gradient fraction. (*b*) Analysis of the gradient fractions for the presence of β-COP and ARF by SDS/PAGE and subsequent immunoblotting using their respective antibodies. (*c*) Irradiation of the gradient fractions and subsequent analysis of crosslink products by SDS/PAGE and autoradiography. (*d*) Analysis of gradient fractions by SDS/PAGE and autoradiography without prior irradiation.

illuminated and analyzed by SDS/PAGE and autoradiography (Fig. 5*c*). The 120-kDa crosslink product appeared in fractions 7–9, coincident with COPI-coated vesicles (see Fig. 5*b*). The appearance of other radioactive bands at about 100 kDa (Fig. 5*c*, lanes 11–13) is regarded nonspecific as they are also obtained in a control experiment without illumination (Fig. 5*d*). Quantitation of the radioactivity by use of a PhosphorImager reveals that the crosslink efficiency in vesicles (0.38% of the [^{35}S]Met-ARF-(Tmd)Phe-82 shifts to the 120-kDa band) does not significantly differ from that on Golgi membranes (0.30%, Fig. 3).

DISCUSSION

To our knowledge, this is the first evidence of a direct and GTP-dependent interaction of coatomer with a defined component on the Golgi membrane and COPI-coated vesicles. Use of the nonhydrolyzable analog of GTP, GTP[γS], allows the accumulation of an intermediate state of the COPI-coated vesicles (33). Under more physiological conditions, where GTP rather then the analog is used, the same but functionally active COPI-coated vesicles can be generated (34), although in much lower yields. From the existence of a specific interaction of β-COP with ARF-GTP[γS] in these vesicles we conclude that ARF represents a structural component of COPI-coated

vesicles. It is of note that the crosslink is only observed when ARF is bound to Golgi membranes. This is in agreement with a postulated conformational change of Golgi-bound ARF upon exchange of GDP for (10), catalyzed by a Golgi-localized nucleotide exchange factor (35, 36). This conformational switch may generate the specific site for interaction with β-COP. Alternatively, the binding site for β-COP might be generated by an oligomerization of membrane-bound ARF-GTP. This is in agreement with several studies showing that for each coatomer complex, more than one ARF molecule is present on COPI-coated vesicles (12, 37).

Recently, a speculative model has emerged that attributes an indirect role of ARF in coatomer recruitment (38, 39). It was suggested that ARF-GTP activates phospholipase D, present on the Golgi membrane, thus inducing vesicle formation and fusion. Our finding of a direct interaction of ARF-GTP[γS] with coatomer does not exclude a regulatory role ARF might play in coatomer binding by activation of phospholipase D. However, this model must be re-evaluated specifically in the light of (*i*) the fact that yeast depleted of phospholipase D activity is viable (40), although coatomer is essential (3, 25, 41, 42) and (*ii*) our finding that a direct interaction of coatomer with ARF exists in purified COPI-coated vesicles.

Recently, a type I membrane protein (p23) was characterized as a Golgi-specific coatomer receptor (37). P23 belongs to the p24 family of proteins that share short C-terminal KKXX-COOH tails and large luminal domains. The dibasic motif has been shown to bind to the α-β′-ε subunits of coatomer as well as to the γ-subunit (7, 8). The KKXXX-COOH present in p23 binds with similar affinity to coatomer as compared with the KKXX-COOH motif (37). Based on the abundance of p23 and ARF in COPI-coated vesicles it has been speculated that these proteins form a scaffold for efficient coatomer binding, allowing the formation of coated buds (37). Thus, budding seems to involve a bivalent interaction of coatomer with the donor membrane, with β-COP interacting with ARF-GTP, and αβ′ε- and/or γ-COP with the cytosolic tail(s) of coatomer receptor(s).

1. Rothman, J. E. (1994) *Nature (London)* **372,** 55–63.
2. Rothman, J. E. & Wieland, F. T. (1996) *Science* **272,** 227–234.
3. Letourneur, F., Gaynor, E. C., Hennecke, S., Demolliere, C., Duden, R., Emr, S. D., Riezman, H. & Cosson, P. (1994) *Cell* **79,** 1199–1207.
4. Donaldson, J. G., Cassel, D., Kahn, R. A. & Klausner, R. D. (1992) *Proc. Natl. Acad. Sci. USA* **89,** 6408–6412.
5. Palmer, D. J., Helms, J. B., Beckers, C. J., Orci, L. & Rothman, J. E. (1993) *J. Biol. Chem.* **268,** 12083–12089.
6. Orci, L., Palmer, D. J., Amherdt, M. & Rothman, J. E. (1993) *Nature (London)* **364,** 732–734.
7. Cosson, P. & Letourneur, F. (1994) *Science* **263,** 1629–1631.
8. Lowe, M. & Kreis, T. E. (1995) *J. Biol. Chem.* **270,** 31364–31371.
9. Harter, C., Pavel, J., Coccia, F., Draken, E., Wegehingel, S., Tschochner, H. & Wieland, F. (1996) *Proc. Natl. Acad. Sci. USA* **93,** 1902–1906.
10. Amor, J. C., Harrison, D. H., Kahn, R. A. & Ringe, D. (1994) *Nature (London)* **372,** 704–708.
11. Kahn, R. A. (1991) *J. Biol. Chem.* **266,** 15595–15597.
12. Serafini, T., Orci, L., Amherdt, M., Brunner, M., Kahn, R. A. & Rothman, J. E. (1991) *Cell* **67,** 239–253.
13. Wittinghofer, A. (1991) *Trends Biochem Sci* **16,** 383–386.
14. Brunner, J. (1993) *Annu. Rev. Biochem.* **62,** 483–514.
15. High, S., Martoglio, B., Görlich, D., Andersen, S. S. L., Ashford, A. J., Giner, A., Hartmann, E., Prehn, S., Rapoport, T. A.,

Cell Biology: Zhao *et al.*

Proc. Natl. Acad. Sci. USA 94 (1997) 4423

Dobberstein, B. & Brunner, J. (1993) *J. Biol. Chem.* **268,** 26745–26751.

16. Vriend, G. (1990) *J. Mol. Graphics* **8,** 52–56.

17. Tanigawa, G., Orci, L., Amherdt, M., Ravazzola, M., Helms, J. B. & Rothman, J. E. (1993) *J. Cell Biol.* **123,** 1365–1371.

18. Brunner, J. (1993) *Chem. Soc. Rev.* **22,** 183–189.

19. Laemmli, U. K. (1970) *Nature (London)* **227,** 680–685.

20. Beckers, J. M. & Rothman, J. E. (1992) *Methods Enzymol.* **219,** 5–12.

21. Waters, M. G., Serafini, T. & Rothman, J. E. (1991) *Nature (London)* **349,** 248–251.

22. Weiss, O., Holden, J., Rulka, C. & Kahn, R. A. (1989) *J. Biol. Chem.* **264,** 21066–21072.

23. Harter, C., Draken, E., Lottspeich, F. & Wieland, F. T. (1993) *FEBS Lett.* **332,** 71–73.

24. Duden, R., Griffiths, G., Frank, R., Argos, P. & Kreis, T. E. (1991) *Cell* **64,** 649–665.

25. Kyhse Andersen, J. (1984) *J. Biochem. Biophys. Methods* **10,** 203–209.

26. Gerich, B., Orci, L., Tschochner, H., Lottspeich, F., Ravazzola, M., Amherdt, M., Wieland, F. & Harter, C. (1995) *Proc. Natl. Acad. Sci. USA* **92,** 3229–3233.

27. Stenbeck, G., Harter, C., Brecht, A., Herrmann, D., Lottspeich, F., Orci, L. & Wieland, F. T. (1993) *EMBO J.* **12,** 2841–2845.

28. Allan, V. J. & Kreis, T. E. (1986) *J. Cell Biol.* **103,** 2229–2239.

29. Malhotra, V., Serafini, T., Orci, L., Shepherd, J. C. & Rothman, J. E. (1989) *Cell* **58,** 329–336.

30. Helms, J. B., Palmer, D. J. & Rothman, J. E. (1993) *J. Cell Biol.* **121,** 751–760.

31. Pepperkok, R., Scheel, J., Horstmann, H., Hauri, H. P., Griffiths, G. & Kreis, T. E. (1993) *Cell* **74,** 71–82.

32. Donaldson, J. G., Kahn, R. A., Lippincott, S. J. & Klausner, R. D. (1991) *Science* **254,** 1197–1199.

33. Melancon, P., Glick, B. S., Malhotra, V., Weidman, P. J., Serafini, T., Gleason, M. L., Orci, L. & Rothman, J. E. (1987) *Cell* **51,** 1053–1062.

34. Ostermann, J., Orci, L., Tani, K., Amherdt, M., Ravazzola, M., Elazar, Z. & Rothman, J. E. (1993) *Cell* **75,** 1015–1025.

35. Donaldson, J. G., Finazzi, D. & Klausner, R. D. (1992) *Nature (London)* **360,** 350–352.

36. Helms, J. B. & Rothman, J. E. (1992) *Nature (London)* **360,** 352–354.

37. Sohn, K., Orci, L., Ravazzola, M., Amherdt, M., Bremser, M., Lottspeich, F., Fiedler, K., Helms, J. B. & Wieland, F. T. (1996) *J. Cell Biol.* **135,** 1239–1248.

38. Liscovitch, M. & Cantley, L. C. (1995) *Cell* **81,** 659–662.

39. Ktistakis, N. T., Brown, H. A., Waters, M. G., Sternweis, P. C. & Roth, M. G. (1996) *J. Cell Biol.* **134,** 295–306.

40. Waksman, M., Eli, Y., Liscovitch, M. & Gerst, J. E. (1996) *J. Biol. Chem.* **271,** 2361–2364.

41. Duden, R., Hosobuchi, M., Hamamoto, S., Winey, M., Byers, B. & Schekman, R. (1994) *J. Biol. Chem.* **269,** 24486–24495.

42. Faulstich, D., Auerbach, S., Orci, L., Ravazolla, M., Wegehingel, S., Lottspeich, F., Stenbeck, G., Harter, C., Wieland, F. T. & Tschochner, H. (1996) *J. Cell Biol.* **135,** 53–61.